Geoscience Frontiers xxx (2016) 1–12

HOSTED BY

ELSEVIER

Contents lists available at ScienceDirect

China University of Geosciences (Beijing)

Geoscience Frontiers

journal homepage: www.elsevier.com/locate/gsf

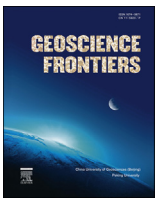

Research paper

Late Paleozoic to Mesozoic extension in southwestern Fujian Province, South China: Geochemical, geochronological and Hf isotopic constraints from basic-intermediate dykes

Sen Wang [a,c], Da Zhang [a,*], Ganguo Wu [a], Absai Vatuva [a], Yongjun Di [a], Pengcheng Yan [a], Haibin Feng [a], Shuai Ma [b]

[a] State Key Laboratory of Geological Processes and Mineral Resources, China University of Geosciences, Beijing, 100083, China
[b] New Brunswick University, Fredericton, New Brunswick, Canada
[c] Beijing Institute of Exploration Engineering, China Geological Survey, Beijing, 100083, China

ARTICLE INFO

Article history:
Received 24 November 2015
Received in revised form
18 May 2016
Accepted 25 May 2016
Available online xxx

Keywords:
Diabase
Late Paleozoic
Extensional tectonics
Southwestern Fujian

ABSTRACT

The tectonic evolution of SE China block since late Paleozoic remains debated. Here we present a new set of zircon U-Pb geochronological, Lu-Hf isotopic data and whole-rock geochemistry for two stages of basic-intermediate dykes from the southwestern Fujian. The samples were collected from the NE-trending (mainly diabases) and NW-trending (mainly diabasic diorites) dykes and yielded zircon U-Pb ages of 315 and 141 Ma, with $\varepsilon_{Hf}(t)$ values of −8.90 to 7.49 and −23.39 to −7.15 (corresponding to T_{DM2} values of 850 to 1890 Ma and 737 to 2670 Ma), respectively. Geochemically these rocks are characterized by low TiO_2 (0.91−1.73 wt.%) and MgO (3.04−7.96 wt.%), and high Al_2O_3 (12.5−16.60 wt.%) and K_2O (0.60−3.63 wt.%). Further they are enriched in LREEs and LILEs (Rb, Ba, Th and K), but depleted in HFSEs (Nb, Ta and Zr). The tectonic discrimination analysis revealed that the dykes were formed in an intraplate extensional environment. However, the NW trending dykes show crust-mantle mixed composition, which indicate an extensional tectonic setting with evidence for crustal contamination. The SE China block experienced two main stages of extensional tectonics from late Carboniferous to early Cretaceous. The tectonic evolution of the SE China block from late Devonian to Cretaceous is also evaluated.

1. Introduction

The southwestern Fujian area, located on the southeastern margin of South China block in the Eurasian plate, is well-known for the occurrence of large-scale iron polymetallic ore deposits, such as the Makeng and Zijinshan deposits. The Zhenghe-Dapu and Nanping-Ninghua fault, a late Paleozoic depression zone in Fujian Province, limits the eastern and the northern border of this region. Earlier studies identified four major tectono-magmatic events in SE China block following its formation: the Caledonian (middle Paleozoic), Variscan (middle Devonian–early Permian), Indosinian (Triassic) and Yanshanian (Jurassic–Cretaceous) events (Li and Li, 1988; Chen et al., 1999; Mao et al., 2003; Wang and Li, 2003; Wang et al., 2007a, b, 2010, 2011; Xu et al., 2013a, b; Zhang et al., 2013). Voluminous igneous rocks formed during these events (Mao et al., 2002, 2006; Wang et al., 2007a; Xu et al., 2013a). Several previous studies have addressed the Mesozoic magmatism and its relationship to the tectonic environment. A few works also report the widespread basic-intermediate dykes in southwestern Fujian, which are spatially associated with 'Makeng-type' iron deposits.

Previous studies on the late Paleozoic sedimentary environment report signatures of extensional tectonics in the SE China block from upper Devonian to upper Permian (Wei et al., 1997; Wang, 2005; Wang et al., 2009; Lin, 2011). Wei et al. (1997) suggested that SE China block was located in a marine basin margin environment from late Devonian to Permian. Wang (2005) studied the volcanic rocks in the Shanghang-Dehua area and suggested the existence of a marine extensional tectonic environment during Carboniferous. Wang et al. (2009) argued that southwestern Fujian was located in a passive continental margin setting during the late Paleozoic. However, information on the late Paleozoic extensional setting for this region based on geochronological studies is limited. In this paper, we

* Corresponding author. Tel.: +86 01082322395.
E-mail address: zhangda@cugb.edu.cn (D. Zhang).
Peer-review under responsibility of China University of Geosciences (Beijing).

http://dx.doi.org/10.1016/j.gsf.2016.05.005

present new geochronological and geochemical data to evaluate the late Paleozoic extensional tectonics in SE China block.

The late Mesozoic extensional tectonics in SE China has been correlated to the tectonic shift from EW-trending Paleo-Tethys structural domain to an NE–SW-trending tectonic system across the Pacific in the early–middle Jurassic (Li, 2000; Wu et al., 2000; Mao et al., 2002; Zhang et al., 2004; Wang et al., 2015). The upper Mesozoic mafic rocks and I-type granites, formed in the extensional setting, are widespread in coastal areas of SE China block which have been dated as 90–101 Ma (Dong et al., 2010; Tang et al., 2010; Yang et al., 2010; Jiang et al., 2013). However, the precise time of initiation of extensional tectonics is unclear.

Mafic dyke swarms are typical indicators of regional extensional setting (Hou et al., 2006a, b; Peng et al., 2008; Wang et al., 2013; Wu et al., 2014). Therefore, the widespread basic-intermediate dykes can provide important evidence for extension of southwestern Fujian. This study presents a set of new geochronological and geochemical data from representative diabase dykes from southwestern Fujian and addresses the tectonic evolution and extensional tectonic setting of SE China block.

2. Geological setting

SW Fujian, located in southeastern Cathaysia, is an important part of the Mesozoic Tectonic-Magmatic Zone on the west side of the Pacific (Fig. 1). There are three main types of sedimentary rocks exposed in southwestern Fujian: Pre-Devonian basement rocks, late Paleozoic–middle Triassic clastic sedimentary and cap carbonate strata, and Mesozoic–Cenozoic continental clastic and volcanic rock series (Mao et al., 2001; Zhang et al., 2013). Though all the strata, except for the Silurian and lower Devonian, are exposed, the upper Devonian to upper Mesozoic strata constitute the main sedimentary rocks in the study area. The upper Devonian to middle Triassic strata are the major neritic and paralic clastic sedimentary rocks, consisting of, from bottom to top, pre-Devonian epi-metamorphic detrital rocks, upper Devonian Taozikeng Formation–lower Carboniferous Lindi Formation (D_3t–C_1l) coarse detrital rocks, upper Carboniferous Jingshe Formation–upper Permian Qixia Formation (C_2j–P_2q), and upper Permian Wenbishan Formation-lower Triassic Xikou Formation (P_2w–T_1x) paralic coal and neritic calcareous fine detrital rocks.

As an important part of SE China block, southwestern Fujian region experienced the late Devonian to Permian epicontinental sea sedimentation stage, early Triassic to middle Triassic Indosinian movement stage, late Triassic to middle Jurassic tectonic transformation stage and late Jurassic to early Cretaceous large-scale extension stage (Chen et al., 1999; Wu et al., 2000; Shu et al., 2008; Xu et al., 2013a, b; Wang et al., 2015). The region is characterized by Jurassic nappe structures and Cretaceous extensional structures (Mao et al., 2001; Zhang et al., 2004, 2006). In addition, the study area is traversed by widespread regional faults. Among these faults, the NE- and NW-trending faults are dominant in this area, and the earlier NE-trending faults were mainly cut by NW-trending faults. The regional NW–SE compression resulted in multiple structural deformations and different types of NE–SW-trending faults and folds. Mesozoic nappe structures developed widely in southwestern Fujian and its adjacent areas with the nappe direction from NW to SE. These nappe structures are characterized by older allochthonous rocks (pre-Devonian and early Carboniferous) overlapping the younger (late Carboniferous and Permian) autochthonous rocks (Zhang et al., 2013). Fold structures in the area are mostly NE-trending composite synclines, including the Xuanhe synclinorium, Hufang-Yongding anticlinoria and Datian-Longyan synclinorium (Lv et al., 2014). The widespread basic to intermediate dykes intruded into the cores of these folds and the fissures of the regional faults.

Vigorous magmatic activity occurred in several periods (Caledonian, Indosinian and Yanshanian) resulting in the formation of several intrusions, especially Mesozoic acidic and intermediate-acidic magmatic rocks, which occur widely in southwestern Fujian (Zhang and Zuo, 2014). The shape and distribution of the volcanic basins and intrusions are typically controlled by the NE-trending structures (Zhang et al., 2006). Additionally, many basic to intermediate dykes are exposed in the form of diabase dyke swarms in the study area. These dykes are primarily diabases and diabasic diorites, and they mainly appear along the strike direction (Wang et al., 2015). Individual dykes are typically small, and exhibit a vein-like morphology.

3. Sampling and petrology

The gabbroic diabase and diabasic diorite dykes are well developed in southwestern Fujian Province, and they are mainly located in Makeng, Yanshi and Fushi. Their distribution patterns, shapes and nature are primarily controlled by faults and cracks in the wall rocks. The diabasic diorite dykes can be divided into two main swarms: the early NE-trending and the late NW-trending dyke swarms (Figs. 1 and 2). The diabase dykes show steep angles ($>60^\circ$) and commonly intruded into layers of the lower Carboniferous unit. The NW-trending dykes show dip angles ranging from 20° and 80°, and they intruded into the Carboniferous–Permian layers along fractures. Strike lengths of all dykes are less than 500 m. The later dykes have longer strike lengths and more clear boundaries with their surrounding rocks than the earlier dykes. There is no crosscutting phenomenon observed between the two swarms of dykes, however a skarn zone closely related to the earlier dykes was cut by the later diabase dykes, based on which the diabase dykes were divided into two groups (early-stage and late-stage). The locations of representative samples of D3120-b1 (early-stage) and D3097-b3 (late-stage) are shown in Fig. 1, and the other samples were collected from underground.

The fresh gabbroic diabase rock samples are dark-gray, and altered rocks are dark-green. These samples show ophitic textures with medium to fine grained minerals (Fig. 3a, b) and are composed of plagioclase (50%–60%) and augite (30%–40%) with grain size of 0.5 to 2 mm and minor magnetite, sphene, and apatite. These rocks exhibit ophitic texture in which xenomorphic augite replaces net-like crossed platy plagioclase. The augite, is dark green to green-gray. The plagioclase laths are broad, platy and automorphic with grain size of 1.5 to 2 mm, and show varying degrees of sericitization and chloritization.

The diabasic diorites are gray-green to dark- gray in color and exhibitfine hypautomorphic texture and subhedral structure (Fig. 3c, d). They are composed of plagioclase (55%–65%) and hornblende (20%–30%), with some residual pyroxene, as phenocrysts with grain size of 0.5 to 1 mm. These rocks also contain interstitial quartz (5%), feldspar (<5%) and accessory minerals, including sphene and magnetite. The hypidiomorphic elongated plagioclase grains exhibit clear polysynthetic twins and an unusual ring-shaped structure. The xenomorphic granular hornblende grains show obvious pleochroism, and partial tremolitization and chloritization. Xenomorphic quartz typically fill the space between the plagioclase and hornblende grains. The rock samples show evidences of varying degrees of sericitization, chloritization and potassic feldspathization.

4. Analytical methods

4.1. Major and trace elements

Ten fresh whole-rock samples from diabase and diabasic diorite dykes were selected for crushing in an agate mill to 200-mesh after

Please cite this article in press as: Wang, S., et al., Late Paleozoic to Mesozoic extension in southwestern Fujian Province, South China: Geochemical, geochronological and Hf isotopic constraints from basic-intermediate dykes, Geoscience Frontiers (2016), http://dx.doi.org/10.1016/j.gsf.2016.05.005

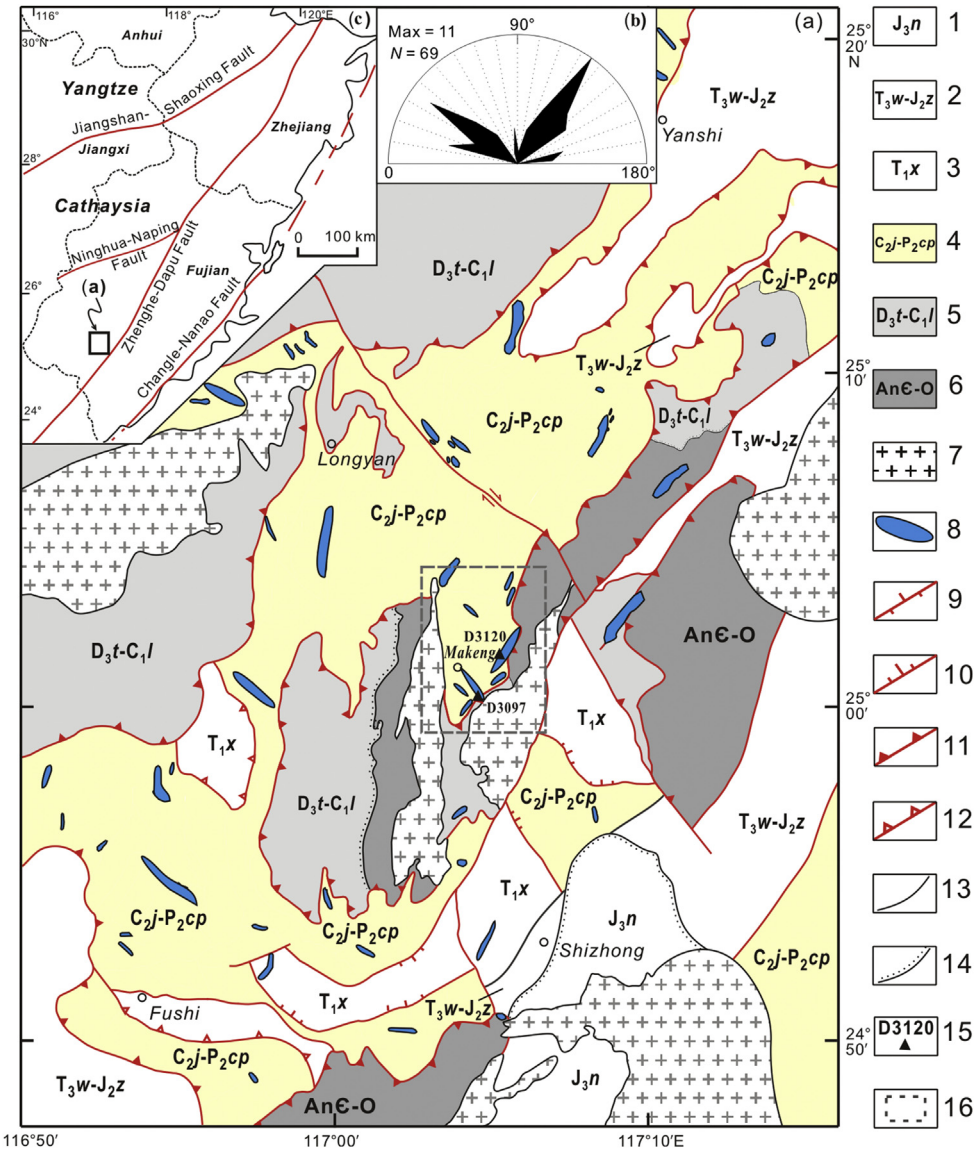

Figure 1. Geological sketch map (a), rose diagram of diabase (b) and tectonic location (c) of the Longyan district, Fujian Province, China. 1. Nanyuan Formation; 2. Wenbinshan-Zhangping Formation; 3. Xikou Formation; 4. Jingshe-Cuipingshan Formation; 5. Taozikeng-Lindi Formation; 6. Precambrian-Ordovician; 7. Yanshanian granites; 8. Basic-intermediate dykes; 9. reversed fault; 10. normal fault; 11. nappe structure; 12. decollement; 13. line of geological limitation; 14. angular unconformity; 15. sampling site; 16. Makeng iron ore district.

the removal of altered surfaces. Major elements were analyzed by X-ray fluorescence spectrometry (XRF; Rigaku RIX 2100 spectrometer) on fused glass disks and trace elements were measured by ICP-MS after acid digestion of the samples in Teflon bombs at the National Research Center for Geoanalysis, Chinese Academy of Geological Sciences, Beijing, China. Rare earth elements (REEs) were analyzed by ICP-MS after REE separation by cation-exchange techniques. The major element data had relative errors of less than 5%. Full details on the analytical procedures can be found in Meng et al. (2014).

4.2. Zircon U-Pb dating

Zircon grains were obtained through a combination of standard heavy liquid and magnetic separation techniques at the Institute of Regional Geology and Mineral Resources Survey of Hebei Province. The zircons were mounted onto an epoxy resin disk, polished to approximately half of the zircon model grain thickness, and documented with both reflected and transmitted light micrographs. Prior to U-Pb isotopic analysis, the internal structures of the zircons were imaged by cathodoluminescence (CL) techniques at the Beijing SHRIMP Centre, Chinese Academy of Geological Sciences, Beijing, China. Analyses of the zircons were conducted using a laser ablation inductively coupled plasma mass spectrometer (LA-ICP-MS) at the Geological Lab Center of the Tianjin Institute of Geology and Mineral Resources. Full details on the LA-ICP-MS analytical procedures are described in Deng et al. (2014). After the analyses, GLITTER 4.4 software was applied to calculate the $^{207}Pb/^{206}Pb$, $^{206}Pb/^{238}U$, $^{207}Pb/^{235}U$ and $^{208}Pb/^{232}Th$ ratios (Van Achterbergh et al., 2001), and common Pb was corrected by using the method from Andersen (2002). Weighted mean U-Pb ages and concordia plots were calculated by using ISOPLOT3.0, with uncertainties quoted at the 1σ and 95% confidence levels (Ludwig, 2003).

4.3. Zircon Lu-Hf isotopes

In situ zircon Hf isotope analyses were obtained from the original locations of the LA-ICP-MS analyses using a Neptune MC-ICP-MS attached to a New Wave UP213 laser ablation microprobe at the

Please cite this article in press as: Wang, S., et al., Late Paleozoic to Mesozoic extension in southwestern Fujian Province, South China: Geochemical, geochronological and Hf isotopic constraints from basic-intermediate dykes, Geoscience Frontiers (2016), http://dx.doi.org/10.1016/j.gsf.2016.05.005

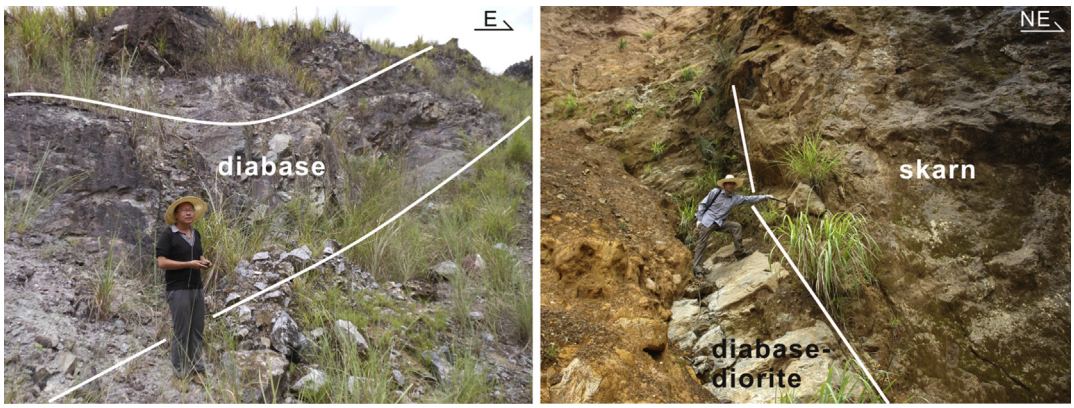

Figure 2. Representative field photographs for the diabase and diabasic diorite dykes in southwestern Fujian.

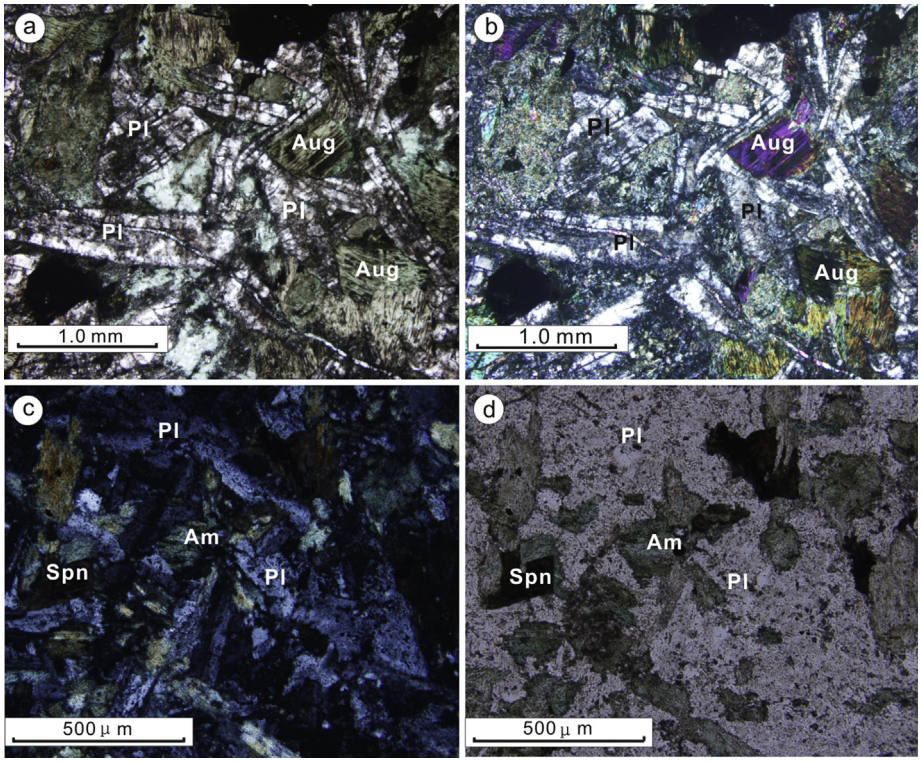

Figure 3. Diabaseic texture of the diabase (a, c–cross-polarized light, b, d–plane-polarized light). Pl–plagioclase; Aug–augite; Am–amphibole; Spn–sphene

Institute of Tibetan Plateau Research, Chinese Academy of Sciences, Beijing, China. The details of the instrumental conditions and data acquisition procedures are given in Wu et al. (2006) and Hou et al. (2007). During the analysis, zircon GJ-1 was used as the external standard, and the Lu–Hf isotopic analyses were performed with a beam diameter of 40 μm and a repetition of 10 Hz. The detailed analytical techniques are well documented by Meng et al. (2014).

4.4. Rb-Sr isotopes

Rb and Sr isotopic compositions of the whole rock samples were determined at Mineral Resources Supervision and Inspection Center of Central South China using an MAT261 TIMS, following the methods of Pu et al. (2004). About 100 mg of the samples was dissolved by the same procedure and used for trace element analyses. The Sr isotopic data are normalized to $^{86}Sr/^{88}Sr = 0.1194$.

5. Results

5.1. Major and trace element geochemistry

The results of the major and trace element analyses for the two groups of diabasic diorites and gabbroic diabase dykes are presented in Table 1. These rocks exhibit similar geochemical features, contain SiO_2 (47.08–57.83 wt.%), TiO_2 (0.91–3.99 wt.%), $K_2O + Na_2O$ (2.63–6.74 wt.%), MgO (1.67–7.96 wt.%), and $Mg^{\#}$ ($Mg^{\#} = Mg/(Mg + Fe^{2+})$; 0.18–0.51). In general, the NE trending dykes show relatively higher MgO and lower SiO_2 than the NW trending ones, indicating their different geochemical composition. As shown in the TAS diagram (Lebas et al., 1986) (Fig. 4a), the plots fall in the field of gabbroic diorite and diorite and belong to the subalkaline series (Irvine and Barager, 1971). In the AMF diagram of Wilson (1989), the samples plot within the tholeiitic series (Fig. 4b).

Please cite this article in press as: Wang, S., et al., Late Paleozoic to Mesozoic extension in southwestern Fujian Province, South China: Geochemical, geochronological and Hf isotopic constraints from basic-intermediate dykes, Geoscience Frontiers (2016), http://dx.doi.org/10.1016/j.gsf.2016.05.005

Table 1
Major element analytical results of the diabase and diabasic diorite dike swarms (wt.%).

Sample	Early dykes				Late dykes						
	400-b10	400-b14	D3120-b1	D3134-b3	7922-b51	7922-b52	7922-b53	7922-b54	D3097-b3	MK-b33	MK-b37
SiO_2	57.41	50.40	47.58	51.59	55.54	54.71	51.47	57.83	57.54	47.08	59.63
TiO_2	1.72	0.99	3.99	0.91	1.72	1.66	1.29	1.62	1.70	3.33	1.47
Al_2O_3	14.63	15.76	11.42	16.60	14.44	14.98	12.50	15.07	13.93	12.55	13.80
Fe_2O_3	2.23	0.97	3.35	3.14	3.73	2.89	6.46	3.04	1.59	2.93	3.28
FeO	5.55	5.99	11.61	6.56	7.06	7.42	9.34	6.25	5.93	9.23	6.01
MnO	0.73	0.20	0.75	0.32	0.16	0.14	0.18	0.14	0.80	0.95	0.24
MgO	3.37	7.96	4.77	5.12	3.82	3.46	4.04	3.04	3.36	3.80	1.67
CaO	5.88	12.85	8.33	6.12	4.09	5.92	5.44	5.42	6.34	12.76	4.11
Na_2O	3.21	2.03	3.18	1.54	1.00	1.84	1.53	3.22	3.07	2.39	3.17
K_2O	3.53	0.59	1.87	2.15	1.82	1.65	1.11	1.22	3.63	1.84	2.96
P_2O_5	0.32	0.11	0.76	0.26	0.29	0.28	0.23	0.29	0.33	1.06	0.57
LOI	1.33	0.14	0.87	0.32	4.86	3.81	4.73	2.59	1.35	0.96	0.24
Total	99.91	97.99	98.48	94.62	98.53	98.76	98.32	99.73	99.57	98.88	97.15
$Mg^{\#}$	0.32	0.51	0.24	0.38	0.29	0.26	0.25	0.27	0.30	0.24	0.18

The REEs and other trace elements data of these rocks are shown in Table 2. The chondrite-normalized patterns of the two groups of basic-intermediate dykes are characterized by light rare earth element (LREE) enrichment, with LREE/HREE ratios varying from 3.87 to 6.82, and $(La/Yb)_N$ values varying between 3.49 and 8.11. These rocks show nearly flat to slightly fractionated chondrite-normalized HREE patterns, relatively high HREE contents and weakly positive Eu anomalies ($\delta Eu = 0.71–1.16$, Fig. 5). These patterns resemble those of intraplate basalt. In the primitive-mantle normalized spider diagram (Fig. 6), some of the samples enriched in large ion lithophile elements (LILEs, such as K, Rb, Ba, Th, etc.) and depleted in high field elements (HFSEs, such as Nb, Ta, Zr, Ti, etc., Fig. 6). They are also characterized by marked Nb, Ta and Ti troughs and Pb peaks in the primitive mantle-normalized incompatible element patterns. These features are distinct from those of mid-oceanic ridge basalts (MORB) and oceanic island basalts (OIB), which are typically characterized by no or insignificant HFSE anomalies (Sun and McDonough, 1989). The low Cr (5.80–64.73 ppm; average 18.78 ppm) and Ni contents (4.22–29.60 ppm; average 11.35 ppm) of the samples, together with their MgO content (1.67–7.96 wt.%; average 4.04 wt.%) indicate that the diabasic diorites and gabbroic diabase were produced from variably fractionated melts and not from primitive magmas.

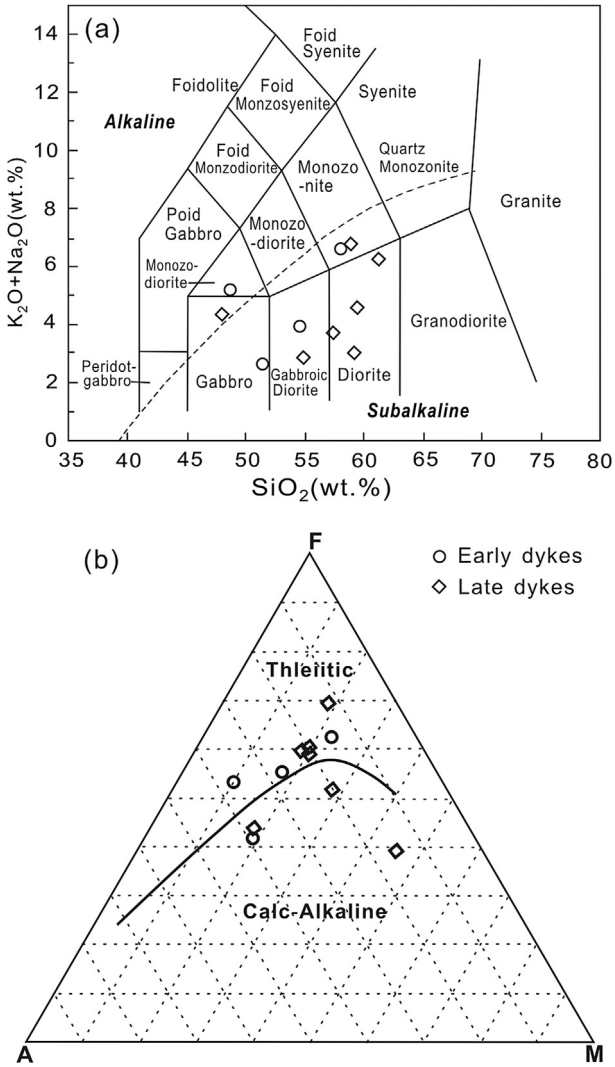

Figure 4. TAS diagram (a) and AFM (ALK-TFe-MgO) diagram (b) of diabase and diabasic diorite dyke swarms.

5.2. Zircon U-Pb and Lu-Hf isotopes

The zircon grains separated from the basic-intermediate dykes (sample D3120-b1 and D3097-b3) are euhedral crystals with lengths of 50 to 80 μm and 70 to 120 μm, respectively. The grains display clear oscillatory zoning without obvious core-mantle structure (Fig. 7). The morphological characteristics of the zircon grains and the magmatic oscillatory zoning indicate that they are magmatic zircons (Belousova et al., 2002).

The zircon U-Pb isotopic analysis results for samples D3120-b1 and D3097-b3 are presented in Table 3. Errors in individual analyses are cited at 1σ, and the weighted mean $^{206}Pb/^{238}U$ ages are quoted at the 95% level of confidence. The $^{206}Pb/^{238}U$ and $^{207}Pb/^{235}U$ ages of some zircons are not concordant possibly because their analyses were performed on inherited cores; these analytical results were excluded from the age calculations. The zircon U-Pb concordia diagrams of samples D3120-b1 and D3097-b3 are shown in Fig. 8. Sample D3120-b1 show consistent U and Th contents with Th/U ratios higher than 0.1 (0.57–1.82), indicating their magmatic origin. In total, 16 of the 17 analyses (#17 was excluded) yielded apparent $^{206}Pb/^{238}U$ ages between 311 ± 3 Ma and 321 ± 2 Ma, with a weighted mean $^{206}Pb/^{238}U$ age of 315.5 ± 1.2 Ma (MSWD = 0.82). Zircons in sample D3097-b3 have Th/U ratios between 0.32 and 6.35 (>0.1), with the U-Pb data clustering near the concordia. Seven of the nine analyses (#1, and

Please cite this article in press as: Wang, S., et al., Late Paleozoic to Mesozoic extension in southwestern Fujian Province, South China: Geochemical, geochronological and Hf isotopic constraints from basic-intermediate dykes, Geoscience Frontiers (2016), http://dx.doi.org/10.1016/j.gsf.2016.05.005

Table 2
REE and trace element analytical results of the diabase and diabasic diabase dike swarms ($\times 10^{-6}$).

Sample	Early dykes				Late dykes						
	400-b10	400-b14	D3120-b1	D3134-b3	7922-b51	7922-b52	7922-b53	7922-b54	D3097-b3	MK-b33	MK-b37
La	36.09	33.72	34.89	25.97	37.41	36.94	29.94	32.48	13.65	18.40	18.10
Ce	76.97	72.11	70.52	48.18	76.80	74.55	59.69	68.08	27.89	50.70	49.20
Pr	9.71	9.13	9.14	6.41	9.46	9.20	7.44	8.59	3.59	7.20	6.74
Nd	38.01	35.93	38.36	26.02	37.74	36.41	29.26	33.24	15.14	35.60	31.40
Sm	7.80	7.48	8.09	4.97	7.92	7.50	5.95	7.04	3.34	9.96	8.35
Eu	2.47	1.95	2.65	1.56	1.84	2.24	1.42	1.71	0.91	3.30	3.24
Gd	7.80	7.36	7.75	4.72	7.96	7.52	5.73	6.86	3.30	10.00	8.68
Tb	1.20	1.16	1.38	0.82	1.31	1.20	0.90	1.09	0.61	1.55	1.28
Dy	7.14	6.72	7.72	4.60	7.61	6.96	5.22	6.52	3.58	9.14	7.71
Ho	1.36	1.29	1.59	0.91	1.51	1.32	1.01	1.25	0.74	1.70	1.43
Er	3.95	3.55	6.17	4.27	4.16	3.83	2.93	3.72	3.67	5.01	4.24
Tm	0.62	0.55	0.70	0.41	0.66	0.61	0.46	0.58	0.34	0.63	0.52
Yb	3.75	3.35	4.02	2.30	3.97	3.69	2.93	3.65	2.12	3.78	3.24
Lu	0.57	0.51	0.70	0.35	0.55	0.51	0.41	0.49	0.31	0.57	0.49
∑REE	197.45	184.81	193.68	131.49	198.90	192.48	153.29	175.31	79.20	157.54	144.62
LREE/HREE	6.48	6.55	5.45	6.15	6.17	6.50	6.82	6.26	4.40	3.87	4.24
$(La/Yb)_N$	6.90	7.22	6.22	8.11	6.76	7.18	7.34	6.38	4.62	3.49	4.01
$(La/Sm)_N$	2.99	2.91	2.79	3.37	3.05	3.18	3.25	2.98	2.64	1.19	1.40
$(Gd/Yb)_N$	1.72	1.82	1.59	1.70	1.66	1.69	1.62	1.55	1.29	2.19	2.22
δEu	0.97	0.80	1.02	0.99	0.71	0.91	0.75	0.75	0.84	1.01	1.16
Sr	642.60	541.10	799.68	617.12	270.00	472.40	316.50	669.50	591.04	578.00	392.00
Rb	216.80	226.20	176.40	147.40	138.50	139.90	91.80	95.60	34.99	158.00	82.10
Ba	780.90	703.40	981.64	771.88	304.20	266.60	152.30	296.90	57.15	111.00	155.00
Th	11.04	10.26	14.19	10.09	10.26	10.14	7.67	9.81	10.39	3.76	2.85
Ta	1.33	1.29	1.88	0.62	1.17	1.21	0.91	1.15	1.05	1.20	1.04
Nb	15.50	16.26	26.57	10.07	15.52	14.30	10.50	12.67	9.76	19.60	16.30
Zr	195.30	200.90	226.30	125.20	193.80	189.00	135.50	190.80	99.70	207.00	167.00
Hf	7.21	7.04	6.95	4.24	5.12	5.03	3.55	5.45	5.73	5.42	4.32
Y	35.66	33.20	38.21	22.22	39.60	36.74	27.47	33.09	18.30	46.50	39.70
U	2.48	2.40	3.43	1.01	2.20	2.18	1.59	2.11	0.93	1.25	1.53
Cs	6.53	5.25	6.02	10.12	5.28	4.48	3.76	2.75	1.96	5.70	1.61
Pb	10.18	12.08	10.93	17.38	11.49	11.22	16.38	6.30	13.91	4.86	2.60
Ga	20.46	18.32	26.19	20.18	20.31	22.67	17.82	22.37	18.54	24.50	23.70
Sc	27.59	28.82	23.56	26.92	31.94	30.38	23.23	30.77	36.14	41.40	43.80
Ni	4.66	4.42	4.22	4.66	8.57	4.25	20.20	8.53	29.60	15.00	20.70
Cr	9.00	10.80	11.70	8.10	5.80	7.50	54.82	16.15	64.73	6.39	11.60
Ta/La	0.04	0.04	0.03	0.03	0.03	0.04	0.08	0.05	0.02	0.07	0.06
Zr/Nb	12.60	12.36	12.49	13.21	12.91	15.06	10.22	8.52	12.43	10.56	10.25

#6 were excluded) yield apparent $^{206}Pb/^{238}U$ ages between 140 ± 1 Ma and 144 ± 1 Ma, with a weighted mean $^{206}Pb/^{238}U$ age of 141.33 ± 0.96 Ma (MSWD = 1.02). Based on the common oscillatory zoning with higher Th/U ratios, we consider 315.5 ± 1.2 Ma and 144 ± 1 Ma to represent the magmatic crystallization ages of the diabase dykes (Corfu et al., 2003).

Zircon Lu-Hf isotope analytical data (10 spots for D3120-b1 and 7 spots for D3097-b3) are presented in Table 4. The Lu-Hf isotopic compositions for the older sample (D3120-b1) exhibit variable initial $^{176}Hf/^{177}Hf$ ratios from 0.282343 to 0.282794 and $\varepsilon_{Hf}(t)$ values between −8.90 and 7.49 (mainly positive values), with T_{DM2} (Hf) values of 850–1890 Ma. The initial $^{176}Hf/^{177}Hf$ ratios for the later diabase sample (D3097-b3) vary from 0.282186 to 0.282891, and its $\varepsilon_{Hf}(t)$ values range from −23.393 to 7.145, corresponding to T_{DM2} values of 737 to 2670 Ma. In the $\varepsilon_{Hf}(t)$-t diagram (Fig. 9), zircons from the sample D3120-b1 plots between the depleted mantle and chondrite Hf isotope evolution lines. The two-stage model ages of the diabase dykes are much larger than their emplacement ages, indicating an enriched mantle source (Wu et al.,

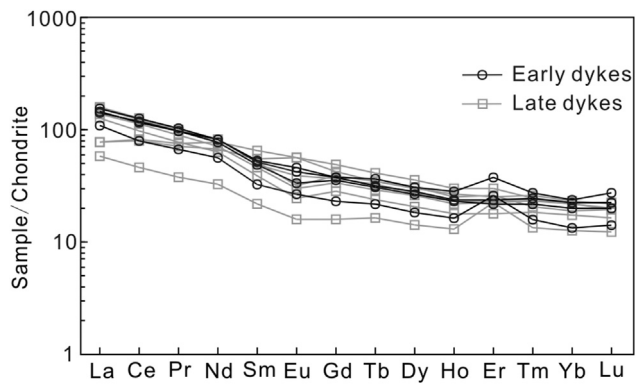

Figure 5. Chondrite-normalized REE patterns of these dyke swarms in the southwestern Fujian (normalization values after Sun S S and Mcdonough W F, 1989).

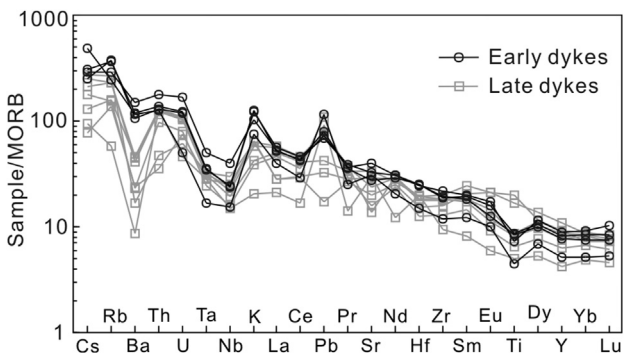

Figure 6. MORB-normalized trace element spider diagram of these dike swarms in the southwestern Fujian (normalized values after Sun S S and Mcdonough W F, 1989).

Please cite this article in press as: Wang, S., et al., Late Paleozoic to Mesozoic extension in southwestern Fujian Province, South China: Geochemical, geochronological and Hf isotopic constraints from basic-intermediate dykes, Geoscience Frontiers (2016), http://dx.doi.org/10.1016/j.gsf.2016.05.005

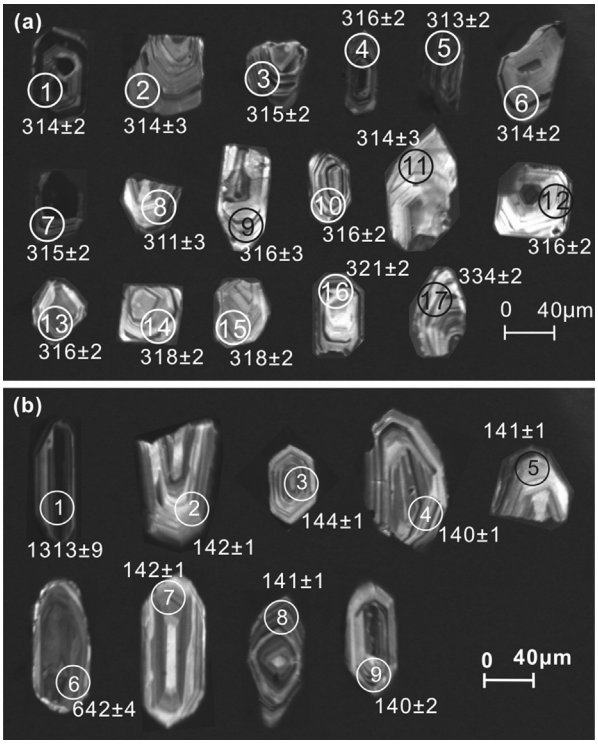

Figure 7. CL images and U-Pb ages (Ma) of the zircons separated from D3120 (a) and D3097 (b).

2006). The data from sample D30970-b3 is dispersed near the chondrite evolutionary line and have a large range of $\varepsilon_{Hf}(t)$ values, indicating that they are possibly derived from a crust-mantle mixed source.

5.3. Rb-Sr isotopes

The initial $^{87}Sr/^{86}Sr$ ratios for the two stages of representative samples were calculated at 315 Ma and 141 Ma respectively. The early stage diabase sample (400-b10) exhibit $^{87}Rb/^{86}Sr$ ratio of 1.0050 and $^{87}Sr/^{86}Sr$ ratio of 0.71258, and the late stage sample (7922-b54) exhibited $^{87}Rb/^{86}Sr$ ratio of 0.3964 and $^{87}Sr/^{86}Sr$ ratio of 0.71090, with calculated initial $^{87}Sr/^{86}Sr$ ratios of 0.70807 and 0.71011 respectively (Table 5).

6. Discussion

6.1. Timing of basic-intermediate dykes and regional magmatism

Mafic magmas generally originate from mantle or lower crust, and are often associated with extensional tectonics. The geochemical data from southwestern Fujian are consistent with an extensional tectonic environment during the late Carboniferous and early Cretaceous (Hou et al., 2006a, b; Peng et al., 2008; Wang et al., 2013; Wu et al., 2014). The U-Pb dating of zircons from the basic-intermediate dykes from this area using LA-ICP-MS yielded weighted mean ages of 315.5 ± 1.2 Ma and 144 ± 1 Ma, which correspond to the late Carboniferous and early Cretaceous, respectively.

As revealed in previous studies, the SW Fujian region and surrounding regions were affected by intra-continental extension during the late Carboniferous and early Cretaceous periods (Wang, 2005; Wu et al., 2005; Zhou et al., 2006; Shu et al., 2009). Although basic-intermediate dykes are widespread in SW Fujian, reports of late Paleozoic magmatism are rare in this area and nearby regions. The only report on the andesitic basalts associated with the Makeng iron ore yielded an Rb-Sr age of 364 Ma, and these basalts are proposed to be derived from a regional extensional tectonic environment (Li and Li, 1988; Wang, 2005).

Table 3
LA-MC-ICPMS Zircon U-Pb analytical results for samples D3097 and D3120.

Spot	Th/U	Isotopic ratios						Age (Ma)					
		$^{207}Pb/^{206}Pb$	1σ	$^{207}Pb/^{235}U$	1σ	$^{206}Pb/^{238}U$	1σ	$^{207}Pb/^{206}Pb$	1σ	$^{207}Pb/^{235}U$	1σ	$^{206}Pb/^{238}U$	1σ
D3097-01	0.3583	0.1614	0.0014	5.0266	0.0538	0.2259	0.0016	2470	15	1824	20	1313	9
D3097-02	0.8435	0.0577	0.0065	0.1771	0.0203	0.0223	0.0002	519	222	166	17	142	1
D3097-03	0.9728	0.0599	0.0050	0.1861	0.0164	0.0225	0.0002	598	102	173	9	144	1
D3097-04	1.0166	0.0639	0.0048	0.1929	0.0149	0.0219	0.0002	738	126	179	11	140	1
D3097-05	1.2592	0.0685	0.0046	0.2084	0.0147	0.0221	0.0002	885	85	192	8	141	1
D3097-06	0.4181	0.0615	0.0005	0.8880	0.0081	0.1048	0.0007	656	17	645	6	642	4
D3097-07	0.9196	0.0881	0.0049	0.2697	0.0150	0.0222	0.0002	1385	106	242	13	142	1
D3097-08	0.9625	0.0524	0.0016	0.1602	0.0055	0.0222	0.0002	303	74	151	5	141	1
D3097-09	6.3522	0.0739	0.0066	0.2236	0.0232	0.0220	0.0004	1037	67	205	8	140	2
D3097-10	0.3212	0.1553	0.0010	7.5416	0.0645	0.3521	0.0026	2406	11	2178	19	1945	14
D3120-01	1.1648	0.0569	0.0007	0.3920	0.0049	0.0500	0.0004	488	27	336	4	314	2
D3120-02	0.6628	0.0591	0.0022	0.4066	0.0148	0.0499	0.0004	569	79	346	13	314	3
D3120-03	0.9411	0.0568	0.0013	0.3925	0.0089	0.0501	0.0004	484	49	336	8	315	2
D3120-04	0.9819	0.0553	0.0008	0.3823	0.0056	0.0502	0.0004	423	32	329	5	316	2
D3120-05	1.8192	0.0611	0.0018	0.4185	0.0126	0.0497	0.0004	643	63	355	11	313	2
D3120-06	1.0184	0.0551	0.0014	0.3796	0.0101	0.0500	0.0004	416	58	327	9	314	2
D3120-07	1.3092	0.0558	0.0005	0.3856	0.0037	0.0501	0.0004	443	20	331	3	315	2
D3120-08	0.9323	0.0565	0.0023	0.3848	0.0161	0.0494	0.0004	470	90	331	14	311	3
D3120-09	0.8796	0.0550	0.0014	0.3808	0.0103	0.0502	0.0005	414	57	328	9	316	3
D3120-10	0.9916	0.0584	0.0011	0.4050	0.0074	0.0503	0.0004	546	39	345	6	316	2
D3120-11	0.5742	0.0796	0.0041	0.5489	0.0292	0.0500	0.0005	1188	101	444	24	314	3
D3120-12	0.7714	0.0598	0.0020	0.4134	0.0142	0.0502	0.0004	595	72	351	12	316	2
D3120-13	0.7094	0.0561	0.0015	0.3879	0.0105	0.0502	0.0004	455	60	333	9	316	2
D3120-14	0.7149	0.0559	0.0019	0.3906	0.0136	0.0506	0.0004	450	76	335	12	318	2
D3120-15	1.1197	0.0629	0.0017	0.4386	0.0122	0.0505	0.0004	706	58	369	10	318	2
D3120-16	1.2812	0.0527	0.0011	0.3703	0.0084	0.0510	0.0004	315	49	320	7	321	2
D3120-17	0.8070	0.0533	0.0009	0.3903	0.0067	0.0532	0.0004	340	38	335	6	334	2

Comment: parts of the date are from Wang et al., 2015.

Please cite this article in press as: Wang, S., et al., Late Paleozoic to Mesozoic extension in southwestern Fujian Province, South China: Geochemical, geochronological and Hf isotopic constraints from basic-intermediate dykes, Geoscience Frontiers (2016), http://dx.doi.org/10.1016/j.gsf.2016.05.005

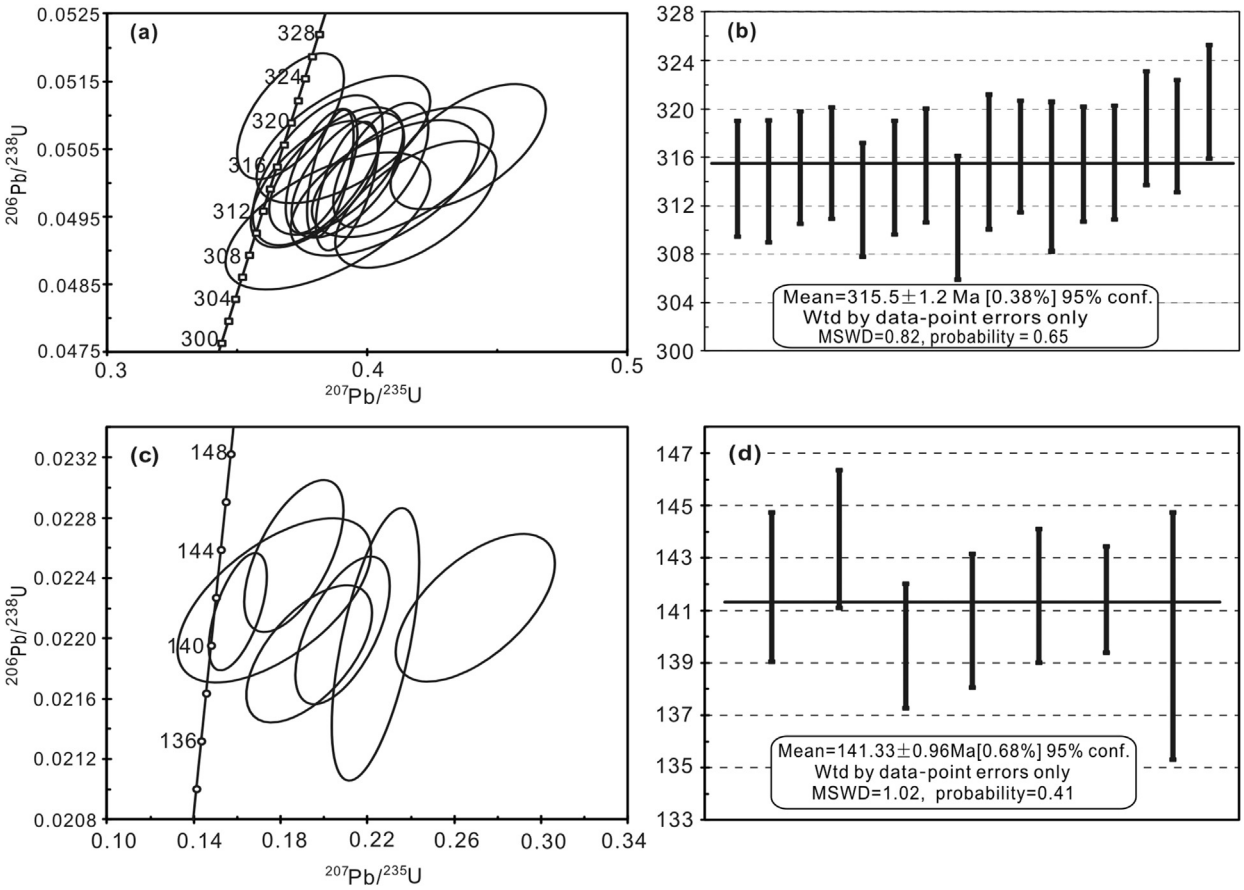

Figure 8. Zircon U-Pb concordia diagrams of samples D3120 (a, b) and D3097 (c, d).

Vigorous Mesozoic magmatism occurred in SW Fujian, especially marked by the emplacement of widespread 130–150 Ma intrusions (Li, 2000; Shi et al., 2009; Li et al., 2010; Li and Jiang, 2014; Zhang and Zuo, 2014; Zhong et al., 2014). Late Mesozoic basic dyke swarms are widespread in SE China, and these rocks were formed in an extensional setting (Zhou and Li, 2000; Sun and Zhou, 2002; Zhang et al., 2004; Dong et al., 2010; Tang et al., 2010; Yang et al., 2010). Additional evidence for extensional tectonic regime includes the upper Mesozoic bimodal volcanic rocks and A-type granites in SW Fujian and its adjacent areas (Ma et al., 1998; Qiu et al., 1999).

6.2. Magmatic source and tectonic indicators

Due to the stability of initial zircon Hf isotopic ratios, they are commonly used as an important tracer for material sources. The

Table 4
Hf isotope composition of zircons from samples D3120 and D3097.

Spot	Age (Ma)	$^{176}Yb/^{177}Hf$	$^{176}Lu/^{177}Hf$	$^{176}Hf/^{177}Hf$	2σ	$\varepsilon_{Hf}(0)$	$\varepsilon_{Hf}(t)$	T_{DM1} (Ma)	T_{DM2} (Ma)	$f_{Lu/Hf}$
D3120-b1										
1	314	0.222057	0.005020	0.282561	0.000096	−7.47	−1.61	1095	1427	−0.85
2	314	0.074232	0.001574	0.282766	0.000036	−0.21	6.37	699	920	−0.95
3	315	0.155193	0.003462	0.282591	0.000048	−6.42	−0.21	1001	1340	−0.90
8	311	0.081402	0.001891	0.282696	0.000035	−2.70	3.75	807	1085	−0.94
10	316	0.157500	0.003237	0.282343	0.000053	−15.16	−8.90	1364	1890	−0.90
11	314	0.083360	0.001515	0.282732	0.000042	−1.40	5.20	746	995	−0.95
12	316	0.058520	0.001065	0.282794	0.000029	0.77	7.49	651	850	−0.97
14	318	0.094445	0.001724	0.282714	0.000043	−2.05	4.59	777	1038	−0.95
15	318	0.088254	0.002209	0.282668	0.000037	−3.68	2.84	855	1148	−0.93
16	321	0.150310	0.003447	0.282547	0.000058	−7.97	−1.66	1067	1436	−0.90
D3097-b3										
3	142	0.047762	0.000927	0.282829	0.000033	2.00	5.03	599	874	−0.97
4	144	0.080587	0.002167	0.282723	0.000146	−1.75	1.20	774	1120	−0.93
5	140	0.075213	0.001421	0.282891	0.000037	4.21	7.14	517	737	−0.96
6	141	0.089123	0.001921	0.282630	0.000048	−5.03	−2.12	903	1329	−0.94
8	142	0.117356	0.003150	0.282186	0.000073	−20.72	−17.91	1593	2328	−0.91
9	141	0.059945	0.001561	0.282412	0.000053	−12.72	−9.77	1204	1815	−0.95
10	140	0.099141	0.003018	0.282032	0.000123	−26.18	−23.39	1813	2670	−0.91

Please cite this article in press as: Wang, S., et al., Late Paleozoic to Mesozoic extension in southwestern Fujian Province, South China: Geochemical, geochronological and Hf isotopic constraints from basic-intermediate dykes, Geoscience Frontiers (2016), http://dx.doi.org/10.1016/j.gsf.2016.05.005

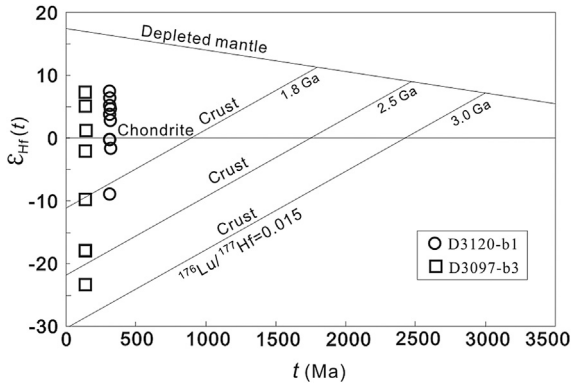

Figure 9. $\varepsilon_{Hf}(t)$-t diagram of samples D3120-b1 and D3097-b3.

two groups of diabase dykes show different Hf isotopic features and $\varepsilon_{Hf}(t)$ and T_{DM2} (Hf) values. The in-situ zircon Lu-Hf isotope analyses from older sample yielded dominantly positive $\varepsilon_{Hf}(t)$ values, reflecting a parental magma that may have been primarily derived from a mantle reservoir, but some negative values may indicate that the magma underwent crust contamination or fluid transformation. The $\varepsilon_{Hf}(t)$ values of the earlier dykes straddle between the depleted mantle and the chondrite Hf isotope evolution lines, and the two-stage model ages of the diabase dykes were much older than their emplacement ages, which indicates that they may be mainly derived from enriched mantle (Wu et al., 2006). The $\varepsilon_{Hf}(t)$ values of younger sample show a wide range from 23.39 to7.14, indicating that these rocks might have been derived from the mixing magmatic source of crust and mantle materials. These two periods of basic-intermediate dykes show a wide range of T_{DM2} (Hf) values that are much older than their zircon crystallization ages, signifying that the primary magma of the basic-intermediate rocks in SW Fujian may have experienced a long residence time after their differentiation from the depleted mantle and the crystallization of the new lower crust. In addition, their whole-rock initial $^{87}Sr/^{86}Sr$ ratios (0.70807 and 0.71011 for early and late dykes, respectively, shown in Table 5) are higher than that of mantle (0.704, after Faure, 1986), but much lower than the average continental crust (0.719, after Sun, 2001). The $(^{87}Sr/^{86}Sr)_i$ value of the two groups of diabase dykes are different: the early stage sample was similar to that of the mantle, suggesting that these rocks may have originated from an enriched mantle with little crustal material contamination; the later stage dyke shows markedly higher initial $^{87}Sr/^{86}Sr$ ratio, indicating a possible mixed crust-mantle source.

The major element patterns of the mafic dykes in SE Fujian exhibit relatively high Si and K and a low Mg, indicating that they have undergone some degree of crystallization differentiation or possibly crustal contamination. These diabasic diorites and gabbroic diabase in SE Fujian are characterized by low Nb and Ta contents and enrichment in LILEs and LREEs, which are representative features of the enriched mantle. These rocks had Zr/Nb ratios of 8.52 to 15.06 (Table 2), which is much higher than that of OIB (5.83) and suggests that they were not derived from an OIB-like asthenospheric mantle. The REE characteristics of the diabases and diabasic diorites, such as the slight negative Eu anomaly and poor HREE fractionation with a $(Dy/Yb)_N$ ranging from 1.78 to 1.81, indicate that fractionation by crystallization of feldspar, olivine or pyroxene was not evident; these characteristics are similar to those of enriched mantle. On the Zr/Y vs. Zr discrimination diagram (Pearce and Norry, 1979) (Fig. 10a), the samples plot in the within-plate basalt field, indicating that these rocks were emplaced in a continental setting, rather than an active arc. In the Ta/Hf vs. Th/Hf discrimination diagram, these rocks plot in the within-plate (continental extensional) basalt field (Wang et al., 2001) (Fig. 10b).

There is no significant difference in the trace element contents between the two groups of diabase dykes, indicating their similar formation environment. The samples in this study exhibit Nb-Ta-Ti negative anomaly on the primitive mantle-normalized diagram with Ta/La ratios (average value of 0.04) lower than the primitive mantle (cf. Ta/La = 0.06, after Wood et al., 1979), indicating that these rocks were derived from a mantle wedge metasomatized by slab-related fluids or contaminated by continental crustal materials (Hawkesworth et al., 1993; Woodhead et al., 1998). The depletion of Nb and Ti in both groups of dykes show features of continental tholeiite. Additionally, some zircon grains show negative $\varepsilon_{Hf}(t)$

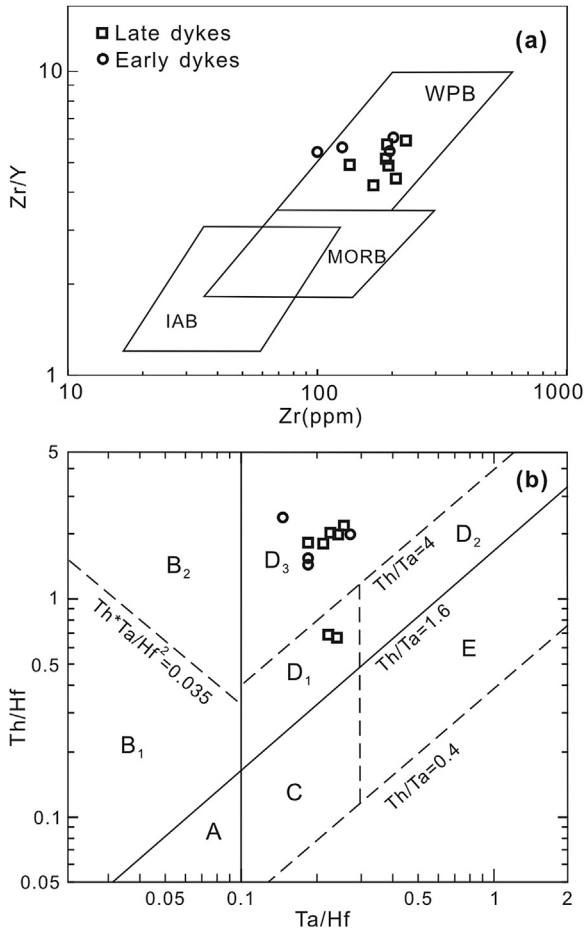

Figure 10. Zr/Y-Zr (a) and Th/Hf-Ta/Hf (b) tectonic discriminant diagrams of the basic-intermediate dike swarms in Longyan. IAB—island arc basalts; MORB—mid ocean ridge basalts; WPB—within plate basalt; A—divergent plate margin; B—convergent plate margin (B_1—oceanic island arc basalts; B_2—continental island arc and continental arc basalts); C—oceanic within plate oceanic island and seamount basalt, T-MORB and T-MORB; D—continental within plate (D_1—intracontinental rift and continental margin rift tholeiite basalts; D_2—intracontinental rift alkaline basalts; D_3—continental extensional zone (or initial rift basalts area); E—mantle plume basalts.

Table 5
Rb-Sr isotopic analytical results of the diabase and diabasic diabase dike swarms.

Sample	Lithology	Rb (ppm)	Sr (ppm)	$^{87}Rb/^{86}Sr$	$^{87}Sr/^{86}Sr$	1σ	$(^{87}Sr/^{86}Sr)_i$
400-b10	Diabase	233.5	670.3	1.005	0.71258	0.00004	0.70807
7922-b54	Diabasic diabase	95.37	693.9	0.3964	0.7109	0.00008	0.71011

Please cite this article in press as: Wang, S., et al., Late Paleozoic to Mesozoic extension in southwestern Fujian Province, South China: Geochemical, geochronological and Hf isotopic constraints from basic-intermediate dykes, Geoscience Frontiers (2016), http://dx.doi.org/10.1016/j.gsf.2016.05.005

values, which support the possibility of continental crustal contamination to some extent. Based on the majorgeochemical features of the basic-intermediate rocks, which include the low Nb-Ta content and the enriched LILEs and LREEs, it can be inferred that the provenance of these rocks could be an enriched mantle source beneath the SW Fujian area. Notably, the overall geochemical characteristics of these rocks are indicative of an enriched lithospheric mantle source, but the early Cretaceous rocks exhibit a small degree of crust-mantle mixing magmatic source.

Generally, the two groups of basic dykes exhibit similar geochemical features, indicating that they originated from an enriched mantle, with some degree of crustal contamination. The later dykes exhibit more obvious crust-mantle mixing magma source, indicating that they experienced stronger crust-mantle interaction.

6.3. Tectonic evolution of SW Fujian

The tectonic evolution of SW Fujian since the late Paleozoic has been a much debated topic. The major process involved a shift from a compressive to an extensional regime since the late Paleozoic, including the significant extensional tectonic stages in the late Devonian–early Triassic and late Jurassic–early Cretaceous (Zhang et al., 2004; Wang, 2005; Wang et al., 2009). The mafic dyke swarms are typically regarded as indications of regional extension (Hou et al., 2006a, b; Peng et al., 2008), and therefore, the 315-Ma and 141-Ma mafic dykes presented in this paper provide important evidence for extensional tectonics in SW Fujian. Based on the geochemical and isotopic analysis we evaluate the late Paleozoic and Mesozoic tectonic evolution of SW Fujian in the following section.

D_3–P_2: Southwestern Fujian was located on the edge of an ocean basin from the late Devonian to late Permian, and a sequence of thick marine and paralic sedimentary strata were deposited. The sedimentary characteristics of the strata indicate that SW Fujian experienced a paraplatform, which formed in the phase of crustal stabilization after the Caledonian orogeny, and formed the continental margin coarse clastic sedimentary rocks since late Devonian due to the regional extension (Wu and Zheng, 1993). The sedimentary characteristics of upper Devonian and lower Carboniferous strata suggest that these rocks formed in a deltaic offshore bar and a distributary river environment, as well as early intra-continental rifting (Bian et al., 1993). The 364 Ma andesitic basalts associated with the Makeng iron ore, currently the earliest mafic magmatic activity reported in SW Fujian, is thought to have formed in regional extensional environment (Wang, 2005). The lower Carboniferous strata are mainly shallow-sea carbonate platform sediments that reflect the gradual expansion of the seawater intrusion from the lower to the upper layers. The consistent deposition of upper Carboniferous carbonate indicates that these rocks formed in a passive continental marginal setting, with characteristics of an extensional epicontinental sedimentary environment (Wu and Zheng, 1993). The NEE-trending bimodal volcanic rocks in Shanghang, Makeng, Pantian, Dehua areas indicate the existence of an extensional tectonic environment during Carboniferous (Wang, 2005). The zircon U-Pb isotopic analysis of the earlier diabase sample yielded a weighted mean $^{206}Pb/^{238}U$ age of 315.5 ± 1.2 Ma, which is similar to the timing of the extensional setting represented by the late Carboniferous sedimentary paleogeographic features. The geochemistry of these rocks is similar to that of the intraplate basalt, indicating that these rocks formed in a continental extensional or intra continental rift setting. In conclusion, it is believed that the SW Fujian experienced strong extension from late Devonian to late Carboniferous, and the extension resulted in crustal thinning and mantle upwelling, and forming the late Carboniferous mafic rocks (including diabase and diabasic diorites; Fig. 11a).

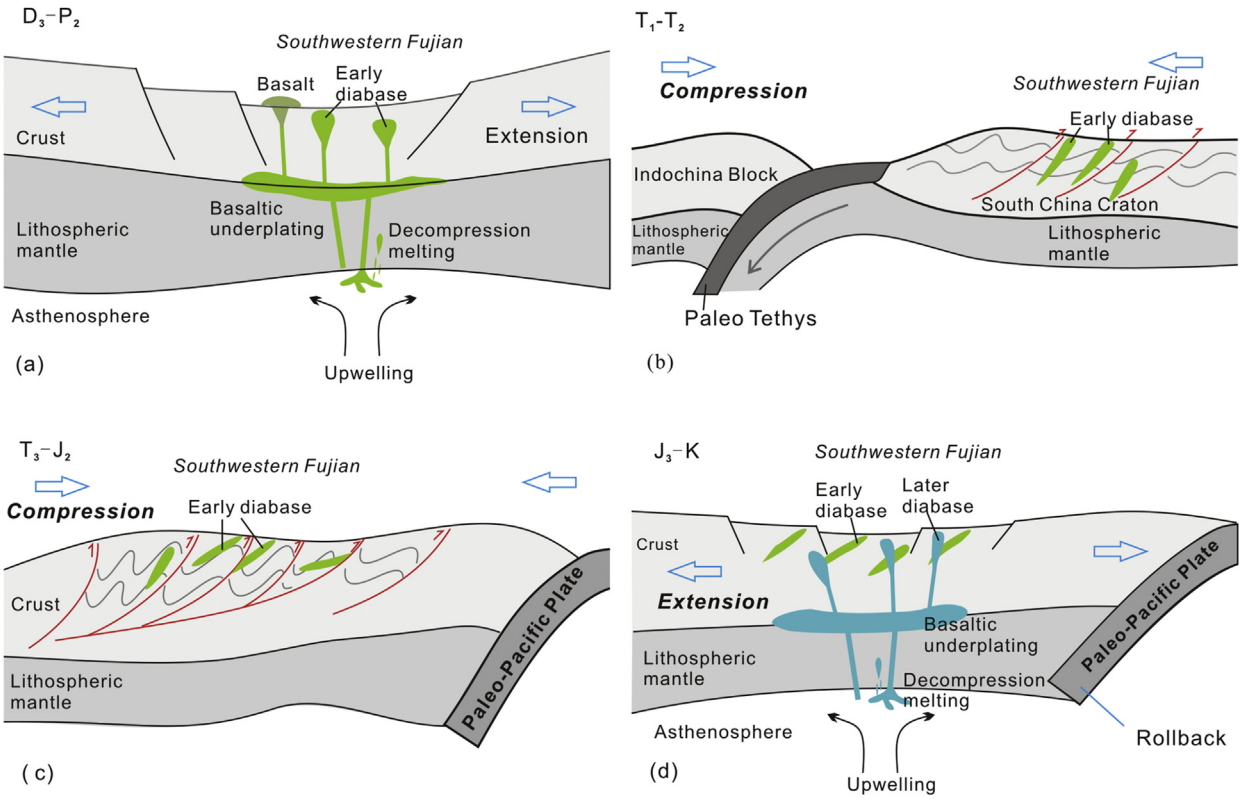

Figure 11. Schematic illustration of the tectonic evolution since the late Paleozoic in southwestern Fujian.

Please cite this article in press as: Wang, S., et al., Late Paleozoic to Mesozoic extension in southwestern Fujian Province, South China: Geochemical, geochronological and Hf isotopic constraints from basic-intermediate dykes, Geoscience Frontiers (2016), http://dx.doi.org/10.1016/j.gsf.2016.05.005

T_1–T_2: Due to the collision between the Yangtze plate and Cathaysia in the early-middle Triassic, SE China developed a Triassic angular unconformity and dextral slipping along NE-trending faults and folds, with N–S-trending orogenic crumpling in the early Mesozoic (Mao, 2013). The late Indosinian plate collision caused widespread folding, thrusting and detachment faults in South China (Zhang et al., 2006), as well as a series of thrusts in southwestern Fujian (Fig. 11b).

T_3–J_2: A transformation of the tectonic framework in South China occurred during the Mesozoic, and the E–W-trending Paleo-Tethys structural domain shifted to a NE-trending tectonic system across the Pacific in the late Triassic–middle Jurassic periods (Wu et al., 2000; Shu, 2012; Zhang et al., 2012). Due to the westward subduction of the Paleo-Pacific plate, deep large-scale thrusting with a NE–SW-trending distribution occurred in southwestern Fujian during the early Yanshanian. The NW–SE-trending compression led to older layers, including pre-Devonian metamorphic rocks and related Caledonian and Indosinian intrusions, uncomfortably overlying Mesozoic strata (Fig. 11c).

J_3–K: Following the early Yanshanian orogeny, a new stage of extension occurred in SW Fujian from the end of the late Jurassic to the early Cretaceous. This extension was induced by deep lithospheric delamination, which led to the upper mantle upwelling and basaltic invasion. By this time, the westward subduction of the Paleo-Pacific plate under South China had slowed or ceased, and formed widespread basins in the Fujian Province. These basins are mostly half-graben-like and controlled by NNE- and NE-trending faults, indicating an extensional setting (Zhang et al., 2006). Early Cretaceous faulted basins and magmatism associated with the extensional setting was widespread in South China, with ages concentrating at approximately 135 ± 5 Ma (Li, 2000; Li et al., 2010). The early Cretaceous volcanic rocks of Nanyuan Formation in Xianyou County yielded show age of 142.3 Ma, indicating an extensional tectonic setting (Xing et al., 2008). Syntectonic granitoid dyke in Guangping area dated 142 ± 1 Ma, representing the end of the NW–SE trending nappe structure and the beginning of the extensional tectonics (Lv et al., 2014). The early Cretaceous A-type granites in Fujian area were regarded as important marks of extensional setting in SE China (Qiu et al., 2000). The LA-ICP-MS zircon U-Pb in this study on the mafic dykes in southwestern Fujian yielded weighted mean $^{206}Pb/^{238}U$ age of 141.33 ± 0.96 Ma. Based on geochronologic and geochemical data, the existence of an early Cretaceous extensional tectonic setting is confirmed. Our data support the widely accepted termination of Pacific subduction, 145 Ma, indicating that the tectonic setting in SW Fujian changed from compression into extension during the latest early Cretaceous (Fig. 11d).

7. Conclusions

(1) The zircon U-Pb dating for two stages of basic-intermediate dykes in southwestern Fujian yielded weighted mean ages of 315.5 and 141.3 Ma, indicating extensional tectonic setting in the SE China block during late Carboniferous and early Cretaceous.

(2) The zircon $\varepsilon_{Hf}(t)$ values of −8.90 to 7.49 and −23.39 to −7.15, corresponding to T_{DM2} values of 850 to 1890 Ma and 737 to 2670 Ma, respectively suggesting that the late Carboniferous mafic dykes were primarily derived from enriched mantle reservoir with limited degree of crustal components, and the early Cretaceous dykes formed from crust-mantle mixing.

(3) The basic-intermediate dykes in southwestern Fujian possess low TiO_2 (0.91–1.73 wt.%), high Al_2O_3 (12.5–16.60 wt.%) and high K_2O (0.60–3.63% wt.%) contents, with $K_2O > Na_2O$. These rocks were enriched in LREEs and LILEs (Rb, Ba, Th and K), depleted in HFSEs (Nb, Ta and Zr). Combining these geochemical features with tectonic discrimination analysis, it is inferred that these mafic dykes formed in an extensional tectonic setting.

(4) Based on the geochemical, isotope geochronologic and sedimentary paleogeographic features, it can be concluded that SE china block experienced two main extensional tectonic stages during late Devonian to Permian and late Jurassic to lower Cretaceous, respectively.

Acknowledgments

This work was supported by projects from the China Geological Survey (Grant Nos. 12120113089600, 12120114028701 and 1212011085472). We are grateful to Mr. Yuan Yuan and Mr. Linkuo Zhang for assistance with the fieldwork.

References

Andersen, T., 2002. Correction of common lead in U-Pb analyses that do not report Pb-204. Chemical Geology 192, 59–79.
Belousova, E.A., Griffin, W.L., O'Reilly, S.Y., Fisher, N.I., 2002. Igneous zircon: trace element composition as an indicator of source rock type. Contributions to Mineralogy and Petrology 143, 602–622.
Bian, X.Z., Chu, Z.X., Zhou, W.D., 1993. Framework of Palaeozoic-Mesozoic tectonic evolution of Fujian Province. Fujian Geology 12, 280–291 (in Chinese).
Chen, P.R., Kong, X.G., Ni, Q.S., Zhang, B.T., Liu, C.S., 1999. Ascertainment and implication of the Early Yianshanian bimodal volcanic associations fron south Jiangxi Province. Geological Review 45, 734–741 (in Chinese).
Corfu, F., Hanchar, J.M., Hoskin, P.W.O., Kinny, P., 2003. Atlas of zircon textures. Zircon 53, 469–500.
Deng, Z.B., Liu, S.W., Zhang, L.F., Wang, Z.Q., Wang, W., Yang, P.T., Luo, P., Guo, B.R., 2014. Geochemistry, zircon U-Pb and Lu-Hf isotopes of an Early Cretaceous intrusive suite in northeastern Jiangxi Province, South China Block: implications for petrogenesis, crust/mantle interactions and geodynamic processes. Lithos 200, 334–354.
Dong, C.W., Yan, Q., Zhang, D.R., Du, Z.Y., Zhu, G.Q., 2010. A petrologic indicator from the Dongji Island mafic dike swarms. Acta Petrologica Sinica 26, 1195–1203 (in Chinese).
Faure, G., 1986. Principles of Isotope Geology, second ed. John Wiley & Sons, New York, pp. 183–199.
Hawkesworth, C.J., Gallagher, K., Hergt, J.M., Mcdermott, F., 1993. Mantle and Slab Contributions in Arc Magmas. Annual Review of Earth and Planetary Sciences 21, 175–204.
Hou, G.T., Liu, Y.L., Li, J.H., 2006a. Evidence for similar to 1.8 Ga extension of the Eastern Block of the North China Craton from SHRIMP U-Pb dating of mafic dyke swarms in Shandong Province. Journal of Asian Earth Sciences 27, 392–401.
Hou, G.T., Wang, C.C., Li, J.H., Qian, X.L., 2006b. Late Paleoproterozoic extension and a paleostress field reconstruction of the North China Craton. Tectonophysics 422, 89–98.
Hou, K.J., Li, Y.H., Zou, T.R., Qu, X.M., Shi, Y.R., Xie, G.Q., 2007. Laser ablation-MC-ICP-MS technique for Hf isotope microanalysis of zircon and its geological applications. Acta Petrol. Sinica 23, 2595–2604 (in Chinese with English abstract).
Irvine, T.N., Barager, W.R.A., 1971. A guide to the chemical classification of the common volcanic rocks. Canadian Journal of Earth Sciences 8 (5), 523–524.
Jiang, S.H., Liang, Q.L., Bagas, L., Wang, S.H., Nie, F.J., Liu, Y.F., 2013. Geodynamic setting of the Zijinshan porphyry-epithermal Cu-Au-Mo-Ag ore system, SW Fujian Province, China: constrains from the geochronology and geochemistry of the igneous rocks. Ore Geology Reviews 53, 287–305.
Lebas, M.J., Lemaitre, R.W., Streckeisen, A., Zanettin, B., 1986. A Chemical Classification of volcanic-rocks based on the Total Alkali Silica Diagram. Journal of Petrology 27, 745–750.
Li, B., Jiang, S.Y., 2014. Geochronology and geochemistry of Cretaceous Nanshanping alkaline rocks from the Zijinshan district in Fujian Province, South China: implications for crust-mantle interaction and lithospheric extension. Journal of Asian Earth Sciences 93, 253–274.
Li, G., Li, H., 1988. Isotopic ages and their regional tectonic significance in Fujian Province. Geology of Fujian 7 (2), 80–118 (in Chinese).
Li, X.H., 2000. Cretaceous magmatism and lithospheric extension in Southeast China. Journal of Asian Earth Sciences 18, 293–305.
Li, X.H., Li, W.X., Li, Q.L., Wang, X.C., Liu, Y., Yang, Y.H., 2010. Petrogenesis and tectonic significance of the similar to 850 Ma Gangbian alkaline complex in South China: evidence from in situ zircon U-Pb dating, Hf-O isotopes and whole-rock geochemistry. Lithos 114, 1–15.
Lin, D.Y., 2011. Research on Tje Late Paleozoic-Triassic Tectonic Evolution and Metallogenetic Regularities of Iron-polymetalic Deposits in the Southwestern Fujian Province. China University of Geosciences, Beijing, pp. 1–147 (in Chinese).
Ludwig, K.R., 2003. Mathematical-statistical treatment of data and errors for Th-230/U geochronology. Uranium-Series Geochemistry 52, 631–656.

Please cite this article in press as: Wang, S., et al., Late Paleozoic to Mesozoic extension in southwestern Fujian Province, South China: Geochemical, geochronological and Hf isotopic constraints from basic-intermediate dykes, Geoscience Frontiers (2016), http://dx.doi.org/10.1016/j.gsf.2016.05.005

Lv, L.J., Zhang, D., Lin, Q.S., et al., 2014. Deformation style and geochronological constraints of Guangping nappe structure in southwest Fujian and its geodynamic significance. Journal of Central South University (Science and Technology) 45, 862–875 (in Chines with English abstract).
Ma, J.Q., He, W.X., Feng, Z.Z., 1998. Features and origin of mesozoic bimodal volcanic rocks in Fujian Province. Regional Geology of China 17, 18–23 (in Chinese).
Mao, J.R., 2013. Mesozoic-cenozoic Magmatism and Mineralization in Southeastern China and the Surrounding Areas. Science Press, Beijing, pp. 1–526 (in Chinese).
Mao, J.R., Chen, R., Li, J.Y., Ye, H.M., Zhao, X.L., 2006. Geochronology and geochemical characteristics of late Mesozoic granotic rocks from southwestern Fujian and their tectonic evolution. Acta Petrologica Sinica 22, 1723–1734.
Mao, J.R., Hu, Q., Xu, N.Z., Xie, F.G., Tai, K.Y., 2003. Geochronology and geochemical characteristics of the Early Mesozoic Tangquan pluton in southwestern Fujian and its tectonic implications. Acta Geologica Sinica-English Edition 77, 361–371.
Mao, J.R., Tao, K.Y., Lee, C.Y., Xie, F.G., Xu, N.Z., 2002. Geochronology and geochemical characteristics in late Mesozoic Sifang pluton, southwestern Fujian, and their significance. Acta Petrologica Sinica 18, 449–458.
Mao, J.R., Tao, K.Y., Xie, F.G., Xu, N.Z., Chen, S.Y., 2001. Rock-forming and ore-forming processes and tectonic environments in Southwest Fujian. Acta Petrologica et Mineralogica 20, 329–336 (in Chinese).
Meng, E., Liu, F.L., Liu, P.H., Liu, C.H., Yang, H., Wang, F., Shi, J.R., Cai, J., 2014. Petrogenesis and tectonic significance of Paleoproterozoic meta-mafic rocks from central Liaodong Peninsula, northeast China: evidence from zircon U-Pb dating and in situ Lu-Hf isotopes, and whole-rock geochemistry. Precambrian Research 247, 92–109.
Pearce, J.A., Norry, M.J., 1979. Petrogenetic implications of Ti, Zr, Y and Nb variations in volcanic rocks. Contributions to Mineralogy and Petrology 69, 33–47.
Peng, P., Zhai, M.G., Ernst, R.E., Guo, J.H., Liu, F., Hu, B., 2008. A 1.78 Ga large igneous Province in the North China craton: the Xiong'er volcanic Province and the North China dyke Swarm. Lithos 101, 260–280.
Pu, W., Zhao, K.D., Ling, H.F., Jiang, S.Y., 2004. High precision Nd isotope measurement by Triton TI mass spectrometry. Acta Geoscientia Sinica 25, 271–274 (in Chinese with English abstract).
Qiu, J.S., Wang, D.Z., Zhou, J.C., 1999. Geochemistry and petrogenesis of the Late Mesozoic bimodal volcanic rocks at Yunshan caldera, Yongtai county, Fujian Province. Acta Petrologica et Mineralogica 18, 2–12 (in Chinese).
Qiu, J.S., Wang, D.Z., Satoshi, K., 2000. Geochemistry and petrogenesis of aluminous A-type granitesin the coastal area of Fujian Province. Geochimica 29 (4), 313–321 (in Chinese).
Shi, J.J., Zhang, D., Wu, G.G., 2009. Re-Os age and geochemistry of the Zhongjia Tin polymetallic deposit and its geological significance in SW Fujian Province, China. Geochimica et Cosmochimica Acta 73. A1209–A1209.
Shu, L.S., 2012. An analysis of principal features of tectonic evolution in South China Block. Geological Bulletin of China 31, 1035–1063 (in Chinese).
Shu, L.S., Faure, M., Wang, B., Zhou, X.L., Song, B., 2008. Late Palaeozoic-Early Mesozoic geological features of South China: response to the Indosinian collision events in Southeast Asia. Comptes Rendus Geoscience 340, 151–165.
Shu, L.S., Zhou, X.M., Deng, P., Wang, B., Jiang, S.Y., Yu, J.H., Zhao, X.X., 2009. Mesozoic tectonic evolution of the Southeast China Block: new insights from basin analysis. Journal of Asian Earth Sciences 34, 376–391.
Sun, S.L., 2001. The Study on Metalogenic Series of Hydrocarbon Alkali-fluids in Devonian in Xicheng Concentrated Mineralization Area, West Qinling, Gansu Province. Chengdu University of Technology, Chengdu, pp. 1–128 (in Chinese).
Sun, S.S., McDonough, W.F., 1989. Chemical and isotopic systematic basalt, implication for mantle composition and processes. Geological Society, Special Publication 42, 313–345.
Sun, T., Zhou, X.M., 2002. Late Mesozoic extension in Southeastern China: petrologic symbols. Journal of Nanjing University 38, 737–746 (in Chinese).
Tang, L.M., Chen, H.L., Dong, C.W., Shen, Z.Y., Cheng, X.G., Fu, L.L., 2010. Late Mesozoic extension in SE China: evidence from the basic dike swarms in Hainan Island, China. Acta Petrologica Sinica 26, 1204–1216 (in Chinese).
Van Achterbergh, E., Ryan, C.G., Jackson, S.E., Griffin, W.L., 2001. Data reduction software for LA–ICP–MS. Laser–Ablation–ICPMS in the earth sciences—principles and applications. Mineralogical Association of Canada Short Course Series 29, 239–243.
Wang, G.S., Ma, W.P., Zhu, W.P., 2009. The Late Paleozoic-Early Triassic sedimentary characteristics and its tectonic significance in southwestern Fujian, China. Journal of Chengdu University of Technology 36, 87–91 (in Chinese).
Wang, J., Li, Z.X., 2003. History of Neoproterozoic rift basins in South China: implications for Rodinia break-up. Precambrian Research 122, 141–158.
Wang, K.X., Sun, T., Chen, P.R., Ling, H.F., Xiang, T.F., 2013. The geochronological and geochemical constraints on the petrogenesis of the Early Mesozoic A-type granite and diabase in northwestern Fujian Province. Lithos 179, 364–381.
Wang, L.J., Yu, J.H., Xu, X.S., Xie, L., Qiu, J.S., Sun, T., 2007a. Formation age and origin of the Gutian-Xiaotao granitic complex in the southwestern Fujian Province, China. Acta Petrologica Sinica 23, 1470–1484.
Wang, S., 2005. On Spatial Distribution and signification of Carboniferous Marine Volcanic Rocks in the Southwest Fujian Depression. Fujian Geology 217–220.
Wang, S., Zhang, D., Lv, L.-j., Absai, V., 2015. The Extensional Tectonic Evolution of the Southwestern Fujian since the Late Paleozoic: constraints from U-Pb Dating and geochemistry of the basic-intermediate dikes. Geotectonica et Metallogenia 39, 889–902 (in Chinese with English abstract).
Wang, Y.J., Fan, W.M., Sun, M., Liang, X.Q., Zhang, Y.H., Peng, T.P., 2007b. Geochronological, geochemical and geothermal constraints on petrogenesis of the Indosinian peraluminous granites in the South China Block: a case study in the Hunan Province. Lithos 96, 475–502.
Wang, Y.J., Zhang, A.M., Fan, W.M., Zhao, G.C., Zhang, G.W., Zhang, Y.Z., Zhang, F.F., Li, S.Z., 2011. Kwangsian crustal anatexis within the eastern South China Block: geochemical, zircon U-Pb geochronological and Hf isotopic fingerprints from the gneissoid granites of Wugong and Wuyi-Yunkai Domains. Lithos 127, 239–260.
Wang, Y.J., Zhang, F.F., Fan, W.M., Zhang, G.W., Chen, S.Y., Cawood, P.A., Zhang, A.M., 2010. Tectonic setting of the South China Block in the early Paleozoic: resolving intracontinental and ocean closure models from detrital zircon U-Pb geochronology. Tectonics 29.
Wang, Y.L., Zhang, C.J., Xiu, X.Z., 2001. Th/Hf - Ta/Hf identification of tectonic setting of basalts. Acta Petrological Sinica 17 (3), 413–421 (in Chinese with English abstract).
Wei, D.G., Jie, Y.J., Huang, T.B., 1997. Regional geological structure of Fujian. Regional Geology of China 16 (2), 162–170 (in Chinese with English abstract).
Wood, D.A., Tarneu, J., Varet, J., Saunders, A.N., Bouhault, H., Joron, J.L., Treuil, M., Cann, J.R., 1979. Geochemistry of basalts drills in the North Atlantic by IPOD Leg49: implications for mantle heterogeneity. Earth and Planetary Science Letters 42, 77–97.
Woodhead, J.D., Eggins, S.M., Johnson, R.W., 1998. Magma genesis in the New Britain island arc: further insights into melting and mass transfer processes. Journal of Petrology 39, 1641–1668.
Wu, C.Z., Santosh, M., Chen, Y.J., Samson, L.M., Lei, R.X., Dong, L.H., Qu, X., Gu, L.X., 2014. Geochronology and geochemistry of Early Mesoproterozoic meta-diabase sills from Quruqtagh in the northeastern Tarim Craton: implications for breakup of the Columbia supercontinent. Precambrian Research 241, 29–43.
Wu, F.Y., Lin, J.Q., Wilde, S.A., Zhang, X.O., Yang, J.H., 2005. Nature and significance of the Early Cretaceous giant igneous event in eastern China. Earth and Planetary Science Letters 233, 103–119.
Wu, F.Y., Yang, Y.H., Xie, L.W., Yang, J.H., Xu, P., 2006. Hf isotopic compositions of the standard zircons and baddeleyites used in U-Pb geochronology. Chemical Geology 234, 105–126.
Wu, G.G., Zhang, D., Chen, B.L., Wu, J.S., 2000. Transformation of Mesozoic tectonic domain and its relation to mineralization in Southeastern China: an evidence of Southwestern Fujian Province. Earth Science 25, 390–396 (in Chinese).
Wu, Q., Zheng, Y.Q., 1993. The sedimentary palaeogeographic analysis of Fujian Province. Fujian Geology 12, 300–319 (in Chinese).
Xing, G.F., Lu, Q.D., Chen, R., Zhang, Z.Y., Nie, T.C., Li, L.M., 2008. Study on the Ending Time of Late Mesozoic Tectonic Regime Transition in South China ——Comparing to the Yanshan Area in North China. Acta Geologica Sinica 82, 451–463 (in Chinese with English abstract).
Xu, Z.J., Cheng, R.H., Wang, L.L., Zhang, L., Shen, Y.J., Yu, Z.F., 2013a. Mineralogical and element geochemical characteristics of the Late Triassic-Middle Jurassic sedimentary rocks in southwestern Fujian Province: constraints on changes of basin tectonic settings. Acta Petrologica Sinica 29, 2913–2924.
Xu, Z.J., Cheng, R.H., Zhang, L., Wang, L.L., 2013b. Transgression-regression event element geochemistry records of southwestern Fujian in Late Triassic-Middle Jurassic. Journal of Central South University 20, 2819–2829.
Yang, Y.F., Dong, C.W., yan, Q., Li, N.M., Zhu, G.Q., Song, Y.Q., 2010. Late Mesozoic extension in coastal area of Zhejiang and Fujian Provinces: an indicator from the basic- intermediate dikes, coastland of Fujian Province. Mineral Petrol 30, 87–94 (in Chinese).
Zhang, D., Gao, T.J., Wu, G.G., Wang, S.X., 2006. Metallogenesis, Deep Process and Potential Assessment of Resources in the Wuyishan-Taiwan Geological Corridorarea. Geological Publishing House, Beijing, pp. 1–179 (in Chinese).
Zhang, D., Wu, G.G., Di, Y.J., Yu, X.Q., Shi, Y.R., Zhang, X.X., Wang, Q.F., Huang, H.J., 2013. SHRIMP U-Pb zircon geochronology and Nd-Sr isotopic study of the Mamianshan Group: implications for the Neoproterozoic tectonic development of southeast China. International Geology Review 55, 730–748.
Zhang, G.S., Wen, H.J., Qiu, Y.Z., 2004. Geochemistry of the late Mesozoic in western Fujian Province. Geochimica 33, 243–253 (in Chinese).
Zhang, Y.Q., Dong, S.W., Li, J.H., Cui, J.J., Shi, W., Su, J.B., Li, Y., 2012. The new progress in the study of Mesozoic tectonics of South China. Acta Geologica Sinica 33, 257–279 (in Chinese).
Zhang, Z.J., Zuo, R.G., 2014. Sr-Nd-Pb isotope systematics of magnetite: implications for the genesis of Makeng Fe deposit, southern China. Ore Geology Reviews 57, 53–60.
Zhong, J., Chen, Y.J., Pirajno, F., Chen, J., Li, J., Qi, J.P., Li, N., 2014. Geology, geochronology, fluid inclusion and H-O isotope geochemistry of the Luoboling Porphyry Cu-Mo deposit, Zijinshan Orefield, Fujian Province, China. Ore Geology Reviews 57, 61–77.
Zhou, X.M., Li, W.X., 2000. Origin of Late Mesozoic igneous rocks in Southeastern China: implications for lithosphere subduction and underplating of mafic magmas. Tectonophysics 326, 269–287.
Zhou, X.M., Sun, T., Shen, W.Z., Shu, L.S., Niu, Y.L., 2006. Petrogenesis of Mesozoic granitoids and volcanic rocks in South China: a response to tectonic evolution. Episodes 29, 26–33.

Please cite this article in press as: Wang, S., et al., Late Paleozoic to Mesozoic extension in southwestern Fujian Province, South China: Geochemical, geochronological and Hf isotopic constraints from basic-intermediate dykes, Geoscience Frontiers (2016), http://dx.doi.org/10.1016/j.gsf.2016.05.005